JACS
JOURNAL OF THE AMERICAN CHEMICAL SOCIETY
Article
pubs.acs.org/JACS

Acylhydrazones as Widely Tunable Photoswitches

Derk Jan van Dijken,[†] Petr Kovaříček,[†,‡] Svante P. Ihrig, and Stefan Hecht*

Department of Chemistry, Humboldt-Universität zu Berlin, Brook-Taylor-Straße 2, 12489 Berlin, Germany

Supporting Information

ABSTRACT: Molecular photoswitches have attracted much attention in biological and materials contexts. Despite the fact that existing classes of these highly interesting functional molecules have been heavily investigated and optimized, distinct obstacles and inherent limitations remain. Considerable synthetic efforts and complex structure−property relationships render the development and exploitation of new photoswitch families difficult. Here, we focus our attention on acylhydrazones: a novel, yet underexploited class of photochromic molecules based on the imine structural motif. We optimized the synthesis of these potent photoswitches and prepared a library of over 40 compounds, bearing different substituents in all four crucial positions of the backbone fragment, and conducted a systematic study of their photochromic properties as a function of structural variation. This modular family of organic photoswitches offers a unique combination of properties and the compounds are easily prepared on large scales within hours, through an atom-economic synthesis, from commercially available starting materials. During our thorough spectroscopic investigations, we identified photoswitches covering a wide range of thermal half-lives of their (*Z*)-isomers, from short-lived T-type to thermally stable P-type derivatives. By proper substitution, excellent band separation between the absorbance maxima of (*E*)- and (*Z*)-isomers in the UV or visible region could be achieved. Our library furthermore includes notable examples of rare negative photochromic systems, and we show that acylhydrazones are highly fatigue resistant and exhibit good quantum yields.

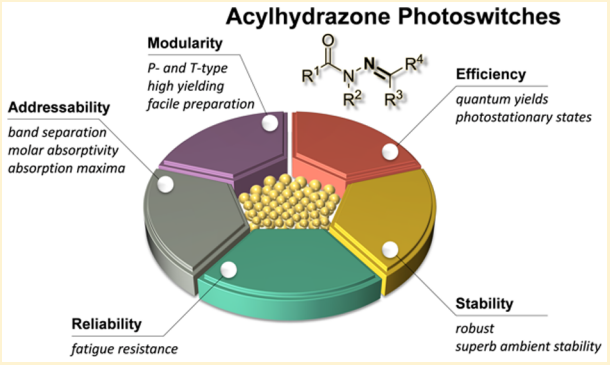

INTRODUCTION

Molecular photoswitches are molecules that can reversibly be converted from one state, or isomer, into another with light. Therefore, the properties of these functional molecules, and potentially the properties of the entire system they are integrated in, can be changed at will. The spatial and temporal precision that light offers is unmatched by any other external stimulus and since it is additionally noninvasive and clean, light and consequently photoswitches have attracted much attention and seen much use over the last decades.[1] Photochromic compounds are most often based on light-induced isomerizations around double bonds or ring-opening and -closing reactions. The ability to modulate a system's intrinsic functions at will, be it due to a change in conjugation, geometry, dipole moment or another property, justifies the enormous amount of effort that has been spent on the development of the field. Consequently, photoswitches now provide an invaluable tool for a large variety of applications in all fields of chemistry; ranging from the interface with biology and biochemistry,[2] supramolecular and organic chemistry,[1,3] materials science,[1,4] all the way to the interface with physics.[5] Over the last decades, however, the assortment of photoswitches that are available has not broadened significantly and the most widely used classes remain stilbenes and azobenzenes,[2a,6] diarylethenes,[3b] and spiropyrans,[7] each bearing intrinsic advantages and limitations.

Photoswitch performance can be assessed through the following performance parameters: *addressability*, *thermal stability*, *efficiency*, and *reliability*. The addressability relates to the maximum absorption wavelength (λ_{max}), the difference in absorption wavelengths between the two different isomers ($\Delta\lambda_{max}$), and the molar absorptivity (extinction coefficient ε), that is, how strong the photoswitch absorbs light of a given wavelength. Efficiency depends on how many photons that are absorbed by the photoswitch are used to induce isomerization of the molecule (quantum yield; Φ) and how high the degree of photoconversion is in the photostationary state (PSS). Thermal stability dictates how long the unstable isomer lives before reverting to the thermodynamically more stable isomer at a given temperature and is measured in thermal half-life $t_{1/2}$, which is the time it takes for half of the molecules to undergo back-isomerization at a given temperature. Depending on the thermal half-life of the less stable isomer, photoswitches are typically classified into T-type or P-type, with the latter exhibiting no (or extremely slow) thermal back isomerization. Finally, reliability is given by the resistance of a molecule to undergo deterioration through undesired side reactions (fatigue resistance) and gives a measure for how often a photoswitch can isomerize without significant degradation.

Received: September 9, 2015
Published: November 18, 2015

DOI: 10.1021/jacs.5b09519
J. Am. Chem. Soc. 2015, 137, 14982−14991

On top of the aforementioned photoswitch-specific properties, more mundane features are additionally required for real-world applications: easy, scalable, and modular synthesis, chemical robustness, and solubility. Note that the rational design of photoswitches is typically challenging and not straightforward, resulting in lengthy syntheses of complicated molecules whose desired properties can not be probed until the final stage.

Inspired by the work of Lehn[8] and Aprahamian,[9] we focused our attention on acylhydrazones. Although hydrazones are structurally related to imines, they possess different features, such as enhanced stability toward hydrolysis in aqueous media, while still offering the possibility of constitutional adaptation via exchange of dynamic covalent bonds.[10] The hydrazone structural motif is used in different fields of chemistry due to its facile synthesis, high stability, and unique structural properties.[11] An interesting feature of this class of molecules is the photochemical, or chemical, $E-Z$ isomerization around the imine-like C═N double bond, changing the configuration and consequently the steric and electronic relation between the moieties on each side of the hydrazone core.[8a] The reverse reaction can be both light-induced (P-type) or heat-induced (T-type), following either an out-of-plane rotation or a nitrogen inversion mechanism.[8d,12] Acylhydrazones present a particularly interesting scaffold, allowing more feasible photochemical isomerization than hydrazones[13] and acylhydrazone photoswitches have proven invaluable in several intriguing applications.[8c,14] However, the systems reported in the literature thus far provide only scattered indications of photochromic properties of this class of compounds.[11b] Therefore, we have undertaken a systematic structure−property relationship study in order to identify the effects of substitution of all four crucial positions of the key backbone fragment (Scheme 1). A sizable library of a novel family of readily

Scheme 1. General Structure and Isomerization of Acylhydrazone Photoswitches

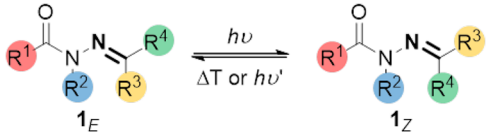

accessible acylhydrazone photoswitches was prepared and crucial characteristics were studied for each of the compounds as a function of systematic changes in their structure.

Isomerization of acylhydrazones induces a configurational change around the C═N double bond, similar to azobenzene-, stilbene-, and (thio)indigo-derived photoswitches. Unlike in azobenzenes,[6a,15] however, the geometry of *both* (*E*)- and (*Z*)-acylhydrazone isomers can be controlled, which can be a major advantage and offers a higher degree of control over their properties. While (thio)indigo-derivatives offer the same advantage, they generally suffer from very poor solubility in most solvents. For structurally related hydrazones, the thermodynamically less-favored (*Z*)-isomer needs to be kinetically stabilized, for example, by introducing an intramolecular H-bonding interaction that can occur in the (*Z*)-isomer.[11b] In other words, to obtain appreciable amounts of (*Z*)-hydrazone, some stabilization is required, imposing substantial structural constraints on the design of these molecules. Furthermore, in comparison, acylhydrazones are more robust and resistant to oxidation, and in addition they are synthetically easily accessible from esters or acyl chlorides via their hydrazide precursors.

The combination of remarkably facile preparation, chemical robustness of precursors and product, as well as the modular approach to the design of acylhydrazones, paves the way to a novel platform of photoswitches with a plethora of tunable "on-demand" properties (Figure 1). By systematically altering and

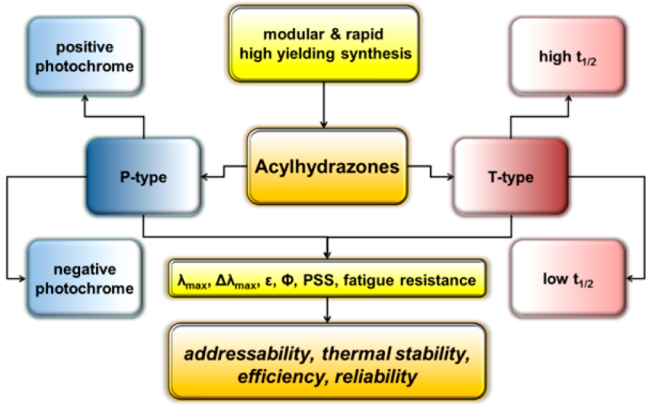

Figure 1. Wide tunability of key properties of acylhydrazone photoswitches through functionalization of the R^1-R^4-positions.

evaluating ample acylhydrazone photoswitches, we have unravelled the connection between structure and switching properties of this emerging family of photochromic compounds and gained access to the rational design of on-demand feature-specific photoswitches. As detailed in the following, we have established guidelines for the custom design of a target photoswitch, which is based on this potent class of photochromic acylhydrazones and exhibits the specific properties needed for the desired goal.

RESULTS AND DISCUSSION

Synthesis. Acylhydrazones can be readily prepared in excellent yields by condensation of a given hydrazide and a carbonyl compound under mild conditions. A wide variety of hydrazides are commercially available at low cost, and the route described in Scheme 2 provides access to an array of acylhydrazone photoswitches in one or two steps, following a fast and high yielding synthesis.

Scheme 2. Optimized Synthesis of Acylhydrazones

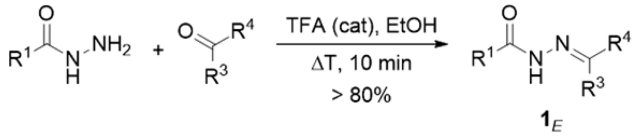

If required, preparation of hydrazides from their corresponding esters is straightforward and can be performed on a large scale. Upon reaction with hydrazine monohydrate in ethanol, esters can be converted into the corresponding pure hydrazides after concentrating the reaction mixtures on a rotary evaporator. For the condensation reaction between any given hydrazide and carbonyl-containing partner of choice, the two are mixed in a 1:1 ratio in ethanol. A catalytic amount of trifluoroacetic acid is added to promote the reaction, and the reaction mixture is heated (typically 10 min) until a clear solution is obtained. When allowed to cool to room

DOI: 10.1021/jacs.5b09519
J. Am. Chem. Soc. 2015, 137, 14982−14991

temperature, the acylhydrazone **1** precipitates from solution and a simple filtration yields the highly pure photoswitch as the (*E*)-isomer in excellent yields (>80%). The reactions are typically performed on a gram scale, yielding several grams of the desired photoswitch, and can easily be further scaled up. Postmodification of the hydrazone backbone is readily accomplished, and, for example, the amide N atom can be methylated with methyl iodide in the presence of sodium hydride. Acylhydrazones showed no sign of degradation after storing them on the bench under ambient conditions for several months, highlighting the robustness of this class of photoswitches.

Acylhydrazone Performance. We first examined the spectral properties of the simplest acylhydrazone **2** (Figure 2a; $R^1 = R^4$ = phenyl, $R^2 = R^3$ = H) by UV/vis spectroscopy

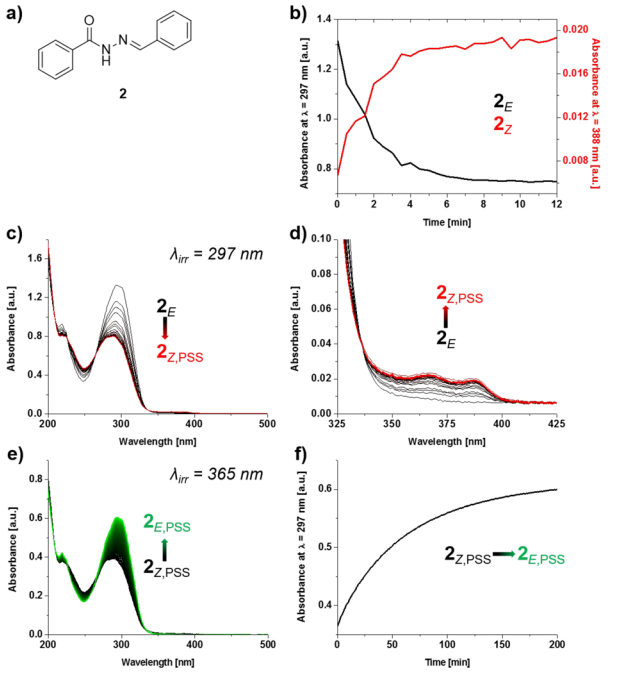

Figure 2. UV/vis absorption spectra upon photoisomerization of parent acylhydrazone photoswitch **2**.[17] (a) Chemical structure of **2**. (b) Absorbance followed at $\lambda_{max}(E)$ = 297 nm (black line) and $\lambda_{max}(Z)$ = 388 nm (red line) over time. (c) Conversion of $\mathbf{2}_E$ (black line) in MeCN (4.43×10^{-5} M) to $\mathbf{2}_{Z,PSS}$ (red line) followed over time under constant irradiation (λ_{irr} = 297 nm, t_{irr} = 11 min); IP at 336 nm. (d) Expansion of (c) of λ = 325–425 nm. (e) Conversion of $\mathbf{2}_{Z,PSS}$ (black line) to $\mathbf{2}_{E,PSS}$ in MeCN (green line, 2.57×10^{-5} M) followed in time (λ_{irr} = 365 nm, t_{irr} = 200 min). (f) Absorbance followed at λ = 297 nm over time as in (e).

(Figure 2). As expected, $\mathbf{2}_E$ displays an absorption band in the UV region (λ_{max} = 295 nm), which upon irradiation (λ_{irr} = 297 nm, t_{irr} = 11 min) decreased while a new weak band at the blue edge of the visible spectrum (λ_{max} = 388 nm) developed (Figure 2b–d), indicating the isomerization to $\mathbf{2}_Z$. Much to our delight, **2** displays a large (54 nm) difference in absorbance maxima of the most bathochromically shifted band between the (*E*)- and (*Z*)-isomers. Good band separation is an important requirement for reversible activation of photoswitches;[1,3e,16] however, it is not a trivial property to foresee or optimize. Irradiation of the (*Z*)-isomer with light of a longer wavelength (Figure 2e,f; λ_{irr} = 365 nm, t_{irr} = 200 min) regenerated the initial (*E*)-isomer, showing that both isomers can be addressed orthogonally; that is, acylhydrazones have good *addressability*.

Clear isosbestic points were observed in both switching directions: the most red-shifted (henceforth denoted as IP) at 336 nm (Figure 2d), suggesting clean conversion from the (*E*)- to the (*Z*)-isomer upon irradiation.[17] The thermodynamically less stable isomer $\mathbf{2}_Z$ reverts to $\mathbf{2}_E$ over time and does not exhibit perfect *thermal stability* and is therefore classified as a T-type photoswitch with a relatively long half-life of the (*Z*)-isomer of $t_{1/2}$ = 145 min at 25 °C. Note that back-isomerization from $\mathbf{2}_Z$ to $\mathbf{2}_E$ (and in fact any other T-type photoswitch reported in this work) can by accelerated by irradiation with light of the appropriate wavelength (Figure 2e,f).

Probing the *efficiency* of acylhydrazone photoswitches was complicated by difficult chromatographic separation of isomers, and quantitative evaluation of photostationary states and consequently determination of quantum yields was only possible for four acylhydrazones reported in this work. We successfully employed ^{1}H NMR measurements to determine the PSS for a selection of photoswitches (Figure 3)[17] and found

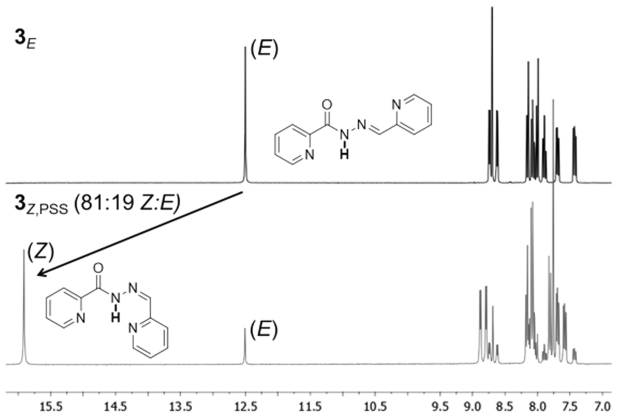

Figure 3. Example ^{1}H NMR spectra for photostationary state determination by integrating the amide N–H for **3** ($R^1 = R^4$ = 2-pyridine). Top: $\mathbf{3}_E$. Bottom: $\mathbf{3}_{Z,PSS}$.

a moderate to good content (51–82%) of (*Z*)-isomer for the investigated acylhydrazones: **3** (81% $\mathbf{3}_z$), **7** (51% $\mathbf{7}_z$), **9** (61% $\mathbf{9}_z$), and **10** (82% $\mathbf{10}_z$). The PSS is reached by irradiation at $\lambda_{max}(E)$ for 5–120 min, depending on the photoswitch. Molar absorptivities are in the order of ε = 15000–20000 $M^{-1}\cdot cm^{-1}$ at λ = 297 or 302 nm and quantum yields for *E* to *Z* isomerization under UV-irradiation (λ_{irr} = 297 or 302 nm) of these photoswitches were calculated to be in the range of $\Phi_{E\rightarrow Z}$ = 0.3–0.4, as obtained from the initial slope of photoconversion (see the Supporting Information for details), which is in good agreement with literature values[13] and places acylhydrazones somewhere between azobenzenes and diarylethenes in terms of efficiency.

A further crucial performance parameter is *reliability*, which describes the fatigue resistance of the photoswitch. While it is generally high for azobenzenes, poor fatigue resistance can be a problem for spiropyrans,[18] while diarylethenes can undergo irreversible oxidation or rearrangement side reactions that give rise to undesired byproducts.[19] We have recently reported general strategies to overcome this important issue for diarylethenes[20] and were interested to study the intrinsic fatigue resistance for acylhydrazone photoswitches (Figure 4). Light was employed to induce the isomerization of T-type

DOI: 10.1021/jacs.5b09519
J. Am. Chem. Soc. 2015, 137, 14982–14991

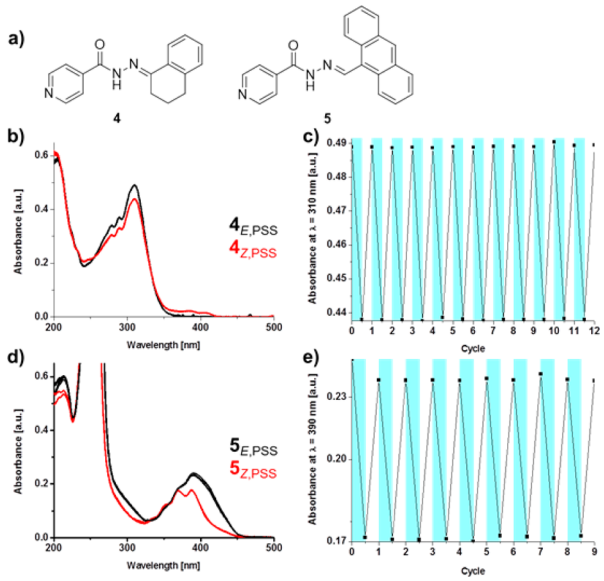

Figure 4. Fatigue resistance of T-type and P-type acylhydrazones. (a) Chemical structure of **4** and **5**. (b) UV/vis absorption spectra of **4** (T-type) in MeCN (2.49×10^{-5} M) during repetitive switching cycles consisting of alternating between $\lambda_{irr}(E \text{ to } Z)$ = 313 nm (t_{irr} = 10 min) and thermal back-isomerization (T = 25 °C, t = 40 min). (c) Corresponding absorbance of $\mathbf{4}_{E,PSS}$ and $\mathbf{4}_{Z,PSS}$ over time as a function of the number of switching cycles followed at $\lambda_{max}(E)$ = 310 nm. (d) UV/vis absorption spectra of **5** (P-type) in MeCN (2.35×10^{-5} M) during repetitive switching cycles consisting of alternating between $\lambda_{irr}(E \text{ to } Z)$ = 405 nm (t_{irr} = 15 min) and $\lambda_{irr}(Z \text{ to } E)$ = 254 nm (t_{irr} = 25 min). (e) Corresponding absorbance of $\mathbf{5}_{E,PSS}$ and $\mathbf{5}_{Z,PSS}$ over time as a function of the number of switching cycles followed at $\lambda_{max}(E)$ = 390 nm. Black line = (*E*)-isomer, red line = (*Z*)-isomer.

acylhydrazone $\mathbf{4}_E$ to $\mathbf{4}_Z$ (Figure 4b, black to red line; λ_{irr} = 313 nm, t_{irr} = 10 min) after which thermal back-isomerization (Figure 4b, red to black line; T = 25 °C, t = 40 min) fully restored $\mathbf{4}_E$. Repetition of these cycles (n = 12) while measuring $\lambda_{max}(E)$ at 310 nm showed no detectable fatigue over time (Figure 4c). Fatigue resistance was furthermore probed at 60 °C and no fatigue could be observed for over 300 cycles (see the Supporting Information). For P-type **5**, both *E* to *Z* and *Z* to *E* isomerization was readily achieved by irradiation with light of different wavelengths (Figure 4d; $\lambda_{irr}(E \text{ to } Z)$ = 405 nm, t_{irr} = 15 min and $\lambda_{irr}(Z \text{ to } E)$ = 254 nm, t_{irr} = 25 min). No fatigue was observed for **5** during nine switching cycles (Figure 4e). Similarly, irradiating samples for an extended duration of time with a powerful 500 W Hg(Xe)-lamp (confirmed for up to 3 h in MeCN) did not give rise to new products as evaluated by UV/vis and ^{1}H NMR spectroscopy, demonstrating that acylhydrazones are highly reliable photoswitches, showing no sign of side product formation upon irradiation.

After refinement of the highly efficient synthesis, we gained access to a large collection of acylhydrazones and prepared over 40 derivatives (see the Supporting Information). The hydrazone linkage divides the variable positions into two sets: R^1 and R^2, stemming from the hydrazide moiety as well as R^3 and R^4, originating from the carbonyl unit (Scheme 1). In the following, we discuss how derivatization of these photoswitches and systematically introducing different substituents in the various positions around the acylhydrazone core influences the performance parameters and properties of this family of photoswitches. We focused our attention on improving the *addressability* of acylhydrazones by bathochromically shifting the wavelength of the most red-shifted absorbance maximum (λ_{max}) while maintaining or further improving the large difference in absorbance maxima between the (*E*)- and (*Z*)-isomers, defined as $\Delta\lambda_{max} = \lambda_{max}(Z) - \lambda_{max}(E)$. Note that shifting the (*Z*)-isomer's absorption bathochromically as compared to the thermally more stable (*E*)-isomer leads to so-called negative photochromism.[22] At the same time, we aimed to reliably influence their *thermal stability*, that is, the absence or presence of a thermal back-reaction (P-type versus T-type) and being able to obtain a variety of different thermal half-lives for the T-type photoswitches.

Acyl Moiety (R^1). The structure of the parent carboxylic acid transfers to the acylhydrazone photoswitch as the R^1-substituent in the hydrazide half. Keeping the carbonyl half for two subsets of switches constant (Scheme 3), several aromatic

Scheme 3. Acylhydrazones Discussed in Table 1

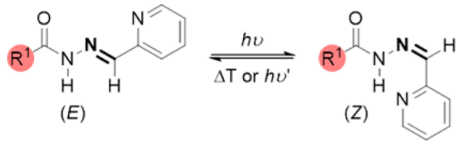

hydrazides were employed in the condensation reaction and the photochromic products were investigated. The results for the first subset, **3** and **6**–**10** (R^2 = R^3 = H, R^4 = 2-pyridine), are summarized in Table 1.

Thermal stabilities for **3** and **6**–**10** are very high, independent of the R^1-substituent and **3** and **6**–**10** are all P-

Table 1. Photochromic Properties of Acylhydrazones Derived from (R^4=) 2-Pyridinecarboxaldehyde, as a Function of Altering the Hydrazide R^1-Moiety (R^2 = R^3 = H)

compd	R^1	λ_{max} [a] [nm]	$\Delta\lambda_{max}$ [b] [nm]	$t_{1/2}$ [c] [min]
6		299	12	stable
7 [d]		301	0	stable
8		334	11	stable
9		292	1	stable
3		301	3	stable
10		305	13	stable

[a]For the (*E*)-isomer. [b]Defined as $\Delta\lambda_{max} = \lambda_{max}(Z) - \lambda_{max}(E)$. [c]At 25 °C; stable photoswitches were defined as those where no thermal *Z*–*E* isomerization was observed for at least 30 min. [d]Insufficient band separation for back-isomerization from *Z* to *E* with light.

DOI: 10.1021/jacs.5b09519
J. Am. Chem. Soc. 2015, 137, 14982–14991

type photoswitches (Table 1), showing no detectable thermal back-reaction for at least 30 min at 25 °C. This can be readily understood, as in the (*Z*)-isomer of these acylhydrazones, the 2-pyridine moiety is perfectly set up to engage in a six-membered intramolecular H-bond with the amide N−H of the hydrazide moiety.[8a] Interestingly, the addressability is barely affected by introducing different R^1-substituents as absorbance maxima for the (*E*)-acylhydrazones are relatively unaffected, except for strongly electron-donating 4-dimethylaminobenzene-derived **8**. Moreover, only a small difference between $\lambda_{max}(Z)$ and $\lambda_{max}(E)$ is observed (13 nm between the two extremes: **7** and **10**). The results of the second subset, **11**−**16** (Scheme 4; $R^2 = R^3 = H$, R^4 = 2-thiophene), where no intramolecular H-bonding is possible, are summarized in Table 2.

Scheme 4. Acylhydrazones Discussed in Table 2

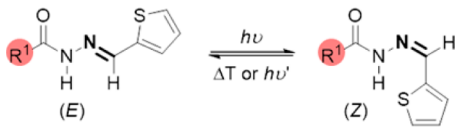

Table 2. Photochromic Properties of Acylhydrazones Derived from (R^4=) 2-Thiophenecarboxaldehyde, as a Function of Altering the Hydrazide R^1-Moiety ($R^2 = R^3 = H$)

compd	R^1	λ_{max} [a] [nm]	$\Delta\lambda_{max}$ [b] [nm]	$t_{1/2}$ [c] [min]
11		319	89	stable
12	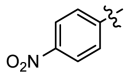	325	76	355
13	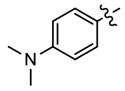	338	84	stable
14		320	91	340
15 [d]		325	0	stable
16		323	90	541

[a]For the (*E*)-isomer. [b]Defined as $\Delta\lambda_{max} = \lambda_{max}(Z) - \lambda_{max}(E)$. [c]At 25 °C; stable photoswitches were defined as those where no thermal *Z*−*E* isomerization was observed for at least 30 min. [d]Despite poor band separation, the shoulder at λ = 265−281 nm allows for back-isomerization from *Z* to *E* with light.

As for the previous subset (Table 1), independent of the R^1-substituent, **11**−**16** all switch upon irradiation and are either P-type photoswitches, or T-type with a long-lived half-life ($t_{1/2}$ > 5 h at 25 °C), displaying high thermal stability. However, the addressability changes as the absorbance maxima for the (*E*)-isomers are higher by ∼20 nm for the (R^4=) 2-thiophene derivatives (Table 2; **11**−**16**) as compared to their (R^4=) 2-pyridine analogues (Table 1; **3** and **6**−**10**). More importantly, the difference in average $\Delta\lambda_{max}$ is very large between the two subsets, bearing identical hydrazide moieties, favoring the (R^4=) 2-thiophene moiety. The effect of the R^1-substituent within this subset is, however, rather modest and the large difference in addressability between the two subsets is due to the different R^4-moiety, which will be discussed hereafter.

Notably, band separation is not a trivial feature for photoswitches that rely on isomerization around a double bond for their switching and while the band separation for the 2-pyridine hydrazones is not satisfactory ($\Delta\lambda_{max}$ = 1−13 nm), it is exceptionally large for the 2-thiophene hydrazones; $\Delta\lambda_{max}$ = 76−91 nm (illustrative example shown in Figure 5). We

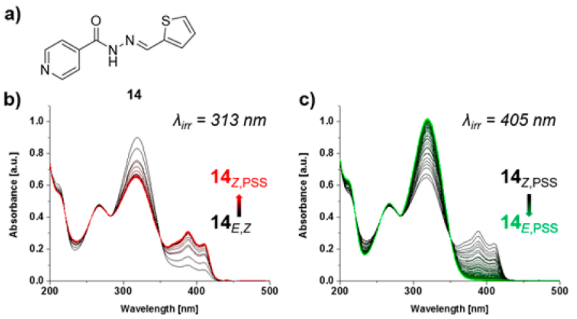

Figure 5. Example UV/vis absorption spectra of R^4 = 2-thiophene derived acylhydrazones. (a) Chemical structure of **14**. (b) MeCN solution of $\mathbf{14}_{E,Z}$ (4.06×10^{-5} M) as synthesized, before (black line) and after (red line) irradiation (λ_{irr} = 313 nm, t_{irr} = 10 min); IP at 351 nm. (c) Photochemical back-isomerization from $\mathbf{14}_{Z,PSS}$ (black line) to $\mathbf{14}_{E,PSS}$ (green line, λ_{irr} = 405 nm, t_{irr} = 45 min), following (b).

hypothesize that both (*E*)- and (*Z*)-isomers of (R^1 =) 2-pyridine-derived acylhydrazones are planar, causing a low $\Delta\lambda_{max}$, while for (R^1=) 2-thiophene the (*Z*)-isomer is nonplanar and hence $\Delta\lambda_{max}$ increases significantly. Furthermore, it was observed that all thiophene-derived acylhydrazones show a typical "fingerprint" triplet in the absorbance spectra of the (*Z*)-isomer around λ = 350−425 nm. The presence of this fingerprint is an indication of structural rigidity and originates from vibronically split bands due to the thiophene C−C vibrations.[21]

We observed that **14** is obtained from the condensation reaction as a mixture of (*E*)- and (*Z*)-isomers (Figure 5b), but can be completely converted to the (*E*)-isomer upon irradiation (Figure 5b,c). A large difference between absorbance maxima is a highly sought after feature for photoswitches and a critical requirement for orthogonal isomerization of P-type photoswitches with light.

Carbonyl Moiety (R^4). The carbonyl moiety is introduced in the acylhydrazone from the carbonyl condensation partner. We investigated the use of various aldehydes, bearing different aromatic moieties that transfer to the photoswitch as the R^4-substituent of the carbonyl half, while keeping the hydrazide moiety constant (Scheme 5; R^1 = 4-pyridine). This set of

Scheme 5. Acylhydrazones Discussed in Tables 3 and 4

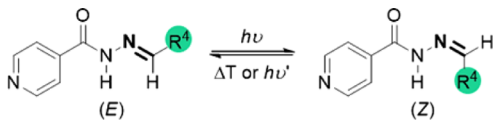

DOI: 10.1021/jacs.5b09519
J. Am. Chem. Soc. 2015, 137, 14982−14991

compounds was divided into three subsets: the first having increasingly large aromatic moieties (Table 3), the second bearing substituents that influence the electronic properties, and the third having different heteroaromatic substituents (Table 4).

Table 3. Photochromic Properties of Acylhydrazones Derived from (R^1 =) 4-Pyridinecarboxylic acid hydrazide, as a Function of Increasing the Aromatic Moiety (R^4) in the Carbonyl Half (R^2 = R^3 = H)

compd	R^4	λ_{max}[a] [nm]	$\Delta\lambda_{max}$[b] [nm]	$t_{1/2}$[c] [min]
17		294	96	4.10
18	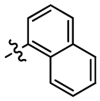	333	-19	139
5	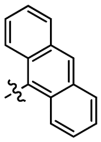	395	-26	stable
19	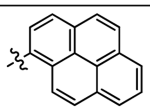	403	-54	stable

[a]For the (*E*)-isomer. [b]Defined as $\Delta\lambda_{max} = \lambda_{max}(Z) - \lambda_{max}(E)$. [c]At 25 °C; stable photoswitches were defined as those where no thermal *Z*–*E* isomerization was observed for at least 30 min.

Aromatic moiety variation in the R^4-position of the acylhydrazone photoswitches has a tremendous effect on both addressability and thermal stability as shown in Table 3. Increasing the size of the aromatic moiety, that is, going from phenyl to naphthyl to anthryl to pyrenyl, extends the conjugated system and consequently increases $\lambda_{max}(E)$ significantly, with a difference of over 100 nm between **17** (R^4 = phenyl) and **19** (R^4 = pyrene). Following the same trend, $\Delta\lambda_{max}$ changes notably as a function of the expanded aromatic system and compound **17** (R^4 = phenyl) displays large band separation ($\Delta\lambda_{max}$ = 96 nm) between the (*E*)- and (*Z*)-isomer. Interestingly, for **18**, **5**, and **19** (R^4 = naphthalene, anthracene and pyrene, respectively) the thermodynamically favored (*E*)-isomer is bathochromically shifted compared to the (*Z*)-isomer ($\Delta\lambda_{max} < 0$), classifying **18**, **5**, and **19** as negative photochromic systems (Figure 6).[22]

Anthracene is well-known to dimerize, but anthracene-derived **5** shows the typical monomer absorbance pattern for both isomers, indicating that switching of the acylhydrazone occurs, rather than dimerization of the anthracene moieties.[23] For **19** (R^4 = pyrene), the trend continues as both **5** and **19** display negative photochromism with increasing band separations of up to -54 nm for **19**. Moreover, the thermal half-life of the (*Z*)-isomer also increases substantially, meaning that while **17** is a T-type photoswitch with one of the lowest thermal half-lives ($t_{1/2}$ = 4.10 min at 25 °C) in our present library, we could not detect a thermal back-reaction for **5** (R^4 = anthracene) and **19** (R^4 = pyrene) at 25 °C. Compound **18** (R^4 = naphthalene) shows intermediate properties, that is, λ_{max} and $t_{1/2}$ increase in the following manner: phenyl < naphthyl < anthryl ≈ pyrenyl. Furthermore, for $\Delta\lambda_{max}$, we find phenyl > naphthyl > anthryl > pyrenyl, demonstrating that switching characteristics can be extrapolated from such structure–property relationships (with due caution), further highlighting the value of our diversity-oriented approach.

Table 4. Photochromic Properties of Acylhydrazones Derived from (R^1 =) 4-Pyridinecarboxylic acid Hydrazide; Scope of heteroaromatic carbonyl R^4-moieties (R^2 = R^3 = H)

compd	R^4	λ_{max}[a] [nm]	$\Delta\lambda_{max}$[b] [nm]	$t_{1/2}$[c] [min]
14		320	91	340
23[d]	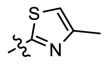	330	0	stable
27[e]		314	109	stable
24		325	80	stable
9[f]		292	1	stable

[a]For the (*E*)-isomer. [b]Defined as $\Delta\lambda_{max} = \lambda_{max}(Z) - \lambda_{max}(E)$. [c]At 25 °C; stable photoswitches were defined as those where no thermal *Z*–*E* isomerization was observed for at least 30 min. [d]Insufficient band separation for back-isomerization from *Z* to *E* with light. [e]The *Z* band is weak, but sufficient for back-isomerization from *Z* to *E* with light. [f]Despite poor band separation, the shoulder at λ = 312–357 nm allows for back-isomerization from *Z* to *E* with light.

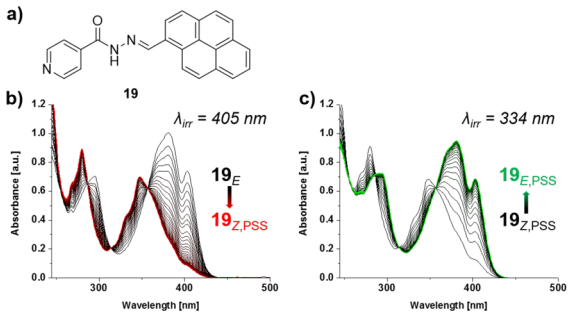

Figure 6. Example UV/vis absorption spectra of an acylhydrazone-based negative photochromic system. (a) Chemical structure of **19**. (b) Solution of $\mathbf{19}_E$ in $CHCl_3$ (2.92×10^{-5} M), before (black line) and $\mathbf{19}_{Z,PSS}$ after (red line) irradiation (λ_{irr} = 405 nm, t_{irr} = 20 min); IP at 356 nm. (c) Photochemical back-isomerization from $\mathbf{19}_{Z,PSS}$ (black line) to $\mathbf{19}_{E,PSS}$ (green line, λ_{irr} = 334 nm, t_{irr} = 15 min), following (b).

Electronic properties of azobenzenes have a large effect on their photochromic behavior,[6a,15,24] and hence, in analogy we investigated the possibility to use substituents with different electronic character as the carbonyl R^4-moiety. For acylhydrazones bearing either electron-withdrawing (**20**, R^4 = 4-nitrophenyl) or -donating (**21** and **22**, R^4 = 4-dimethylamino-

DOI: 10.1021/jacs.5b09519
J. Am. Chem. Soc. 2015, 137, 14982–14991

phenyl and 3,4,5-trimethoxyphenyl, respectively) moieties, large band separations ($\Delta\lambda_{max}$ = 66−86 nm) between the (*E*)- and (*Z*)-isomer were observed. Switching was not inhibited in any way and **20**−**22** are all T-type photoswitches, such as the parent (R^4=) phenyl-compound **17**, with $t_{1/2}$ = 27−47 min.

Heteroaromatic moieties are a common and sometimes even crucial feature in molecular photoswitches[1b,c] and acylhydrazones bearing different heteroaromatic rings in the carbonyl R^4-position were investigated next and the results are summarized in Table 4. All investigated heteroaromatic R^4-substituents (R^1 = 4-pyridine) show an absorbance maximum in the UV region for the (*E*)-isomer (λ_{max} = 292−330 nm). Switching to the (*Z*)-isomer is possible and band separation between both isomers is excellent, $\Delta\lambda_{max}$ = 80−109 nm for **14** (R^4 = 2-thiophene), **27** (R^4 = 2-furan) and **24** (R^4 = 2-pyrrole). However, for **23** (R^4 = 4-Me-2-thiazole) and **9** (R^4 = 2-pyridine) no clear band separation was observed. Fortunately, back-isomerization of $\mathbf{9}_Z$ is possible by irradiation at higher wavelength (λ_{irr} = 334 nm), due to broadening of the absorbance band at λ = 313−355 nm for the (*Z*)-isomer, which holds true for many of the acylhydrazones that have demonstrated poor absolute band separation.[17] Acylhydrazones **23**, **27**, **24**, and **9** show P-type photochromic behavior, while **14** exhibits T-type behavior with a relatively long half-life of $t_{1/2}$ = 340 min at 25 °C. In general, introduction of a heteroaromatic moiety in the R^4-position affects the addressability, in particular $\Delta\lambda_{max}$, but has little effect on the thermal stability.

Aldehyde- or Ketone-Derived Acylhydrazones (R^3). Acylhydrazones can be readily prepared from aldehydes as well as ketones. We expected that introducing a Me-substituent in the R^3-position would induce a change in the addressability of acylhydrazones, due to the increased steric bulk around the C═N double bond. Using methyl ketones as the starting materials in the condensation reaction under the exact same conditions as for the aldehydes, compounds **25**, **26**, and **28** (R^1 = 4-pyridine, R^2 = H, R^3 = CH_3) were prepared in high to excellent yields (60−89%) and their photochromic properties were compared with their aldehyde counterparts (**17**, **27**, and **14**; R^1 = 4-pyridine, R^2 = R^3 = H). The effects on addressability and thermal stability follow the same trends and are examplified by comparing ketone-derived **25** and aldehyde-derived **17** (Figure 7). A large decrease in $\Delta\lambda_{max}$ was observed for **25** (R^4 = phenyl) compared to **17**, which is due to the appearance of a new bathochromically shifted band for the (*Z*)-isomer of the aldehyde-derived acylhydrazone **18** (Figure 7c,e) that is not present for the (*Z*)-isomer of the sterically more hindered ketone-derived analogue **25** (Figure 7b,d).[17]

Furthermore, addressability is generally affected to some extent due to the fact that λ_{max}(*E*) decreases slightly by introduction of a Me-moiety in the R^3-position. And while the thermal stability of **25** ($t_{1/2}$ = 16 min) and **17** ($t_{1/2}$ = 4 min) is in the same range, it is greatly affected for the other two comparisons and $t_{1/2}$ decreases by nearly an order of magnitude for **28** (R^3 = CH_3, R^4 = 2-thiophene) compared to **14** (R^3 = H). Similarly, while **26** (R^3 = CH_3, R^4 = 2-furan) has a thermal half-life of 129 min at 25 °C, **27** (R^3 = H) is a P-type photoswitch (see the Supporting Information).[17]

We subsequently kept the carbonyl half of the acylhydrazones constant (Scheme 6; R^3 = CH_3, R^4 = 2-pyridine) and evaluated the effect of R^3 = CH_3 compared to R^3 = H for different R^1-moieties (Table 5, R^2 = H).

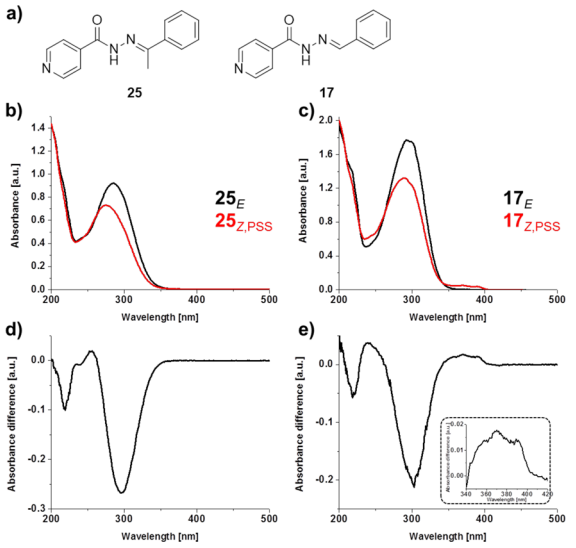

Figure 7. Example UV/vis absorption spectra of R^3 = CH_3 derived acylhydrazones, compared to R^3 = H. (a) Chemical structure of **25** and **17**. (b) Solution of $\mathbf{25}_E$ in MeCN (4.76×10^{-5} M), before (black line) and $\mathbf{25}_{Z,PSS}$ after (red line) irradiation (λ_{irr} = 297 nm, t_{irr} = 25 min). (c) Solution of $\mathbf{17}_E$ in MeCN (7.02×10^{-5} M), before (black line) and $\mathbf{17}_{Z,PSS}$ after (red line) irradiation (λ_{irr} = 297 nm, t_{irr} = 16 min); IP at 342 nm. (d) Difference absorption spectrum of $\mathbf{25}_{Z,PSS}$-$\mathbf{25}_E$. (e) Difference absorption spectrum of $\mathbf{17}_{Z,PSS}$−$\mathbf{17}_E$; inset shows a new band appearing for $\mathbf{17}_Z$ at λ = 340−420 nm.

Scheme 6. Acylhydrazones Discussed in Table 5

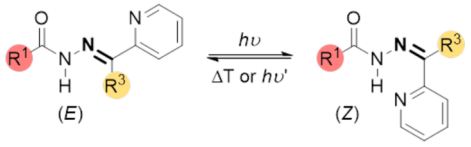

Comparing acylhydrazones with different hydrazide halves (R^1 = 4-pyridine, 2-thiophene, and 4-nitrobenzene, R^2 = H), while keeping the carbonyl half identical (R^3 = CH_3, R^4 = 2-pyridine), showed no significant effects on the photochromic properties between ketone- (R^3 = CH_3) and aldehyde-derived (R^3 = H) acylhydrazones (Table 5) in any case, showing that the R^3-position can be functionalized without inherent loss of photochemical properties and without affecting the changes induced by R^1, thus providing orthogonal handles for optimization of the photoswitches.

***N*-Methylated Acylhydrazones and Steric Strain (R^2 and R^3).** The ability to reversibly switch steric bulk between the different isomers of molecular photoswitches is important in supramolecular chemistry as well as the developing fields of photoswitchable catalysis[3b,f,4d] and photopharmacology.[1c,2c,d,25] Conceptually, many approaches followed in these fields exploit such photoinduced reversible structural changes and hence prompted us to investigate if the introduction of steric interactions (1,3-allylic strain) between the R^2- and R^3-positions would affect the switching capacity of acylhydrazones (Scheme 7). Therefore, two series (R^1 = phenyl or 2-thiophene) of compounds were prepared, where (i) R^2 = R^3 = H (**11** and **16**), (ii) R^2 = CH_3, R^3 = H (**33** and **34**), (iii) R^2 = H and R^3 = CH_3 (**35** and **36**), and (iv) R^2 = R^3 = CH_3 (**37** and **38**). The results are summarized in Table 6.

Exchanging the (R^2) N−H (**11**, **35**, **16**, and **36**) functionality for N−CH_3 (**33**, **37**, **34**, and **38**) causes broadening of all

DOI: 10.1021/jacs.5b09519
J. Am. Chem. Soc. 2015, 137, 14982−14991

Table 5. Photochromic Properties of Acylhydrazones Derived from 2-Acetylpyridine (R^2 = H, R^3 = CH_3, R^4 = 2-pyridine) as a Function of Different (R^1) Hydrazides, Comparing R^3 = CH_3 (29–31) to R^3 = H (9, 10, and 32)

compd	R^1	R^3	λ_{max} [a] [nm]	$\Delta\lambda_{max}$ [b] [nm]	$t_{1/2}$ [c] [min]
29		CH_3	293	17	stable
9		H	292	1	stable
30 [d]		CH_3	303	12	stable
10		H	305	13	stable
31 [e]	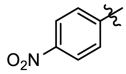	CH_3	292	0	stable
32 [e]	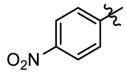	H	297	0	stable

[a]For the (*E*)-isomer. [b]Defined as $\Delta\lambda_{max} = \lambda_{max}(Z) - \lambda_{max}(E)$. [c]At 25 °C; stable photoswitches were defined as those where no thermal *Z*–*E* isomerization was observed for at least 30 min. [d]While an increase in the band at λ = 268 nm is observed, the shoulder at λ = 315–360 nm does not go back thermally. [e]Insufficient band separation for back-isomerization from *Z* to *E* with light.

Scheme 7. Acylhydrazones Discussed in Table 6

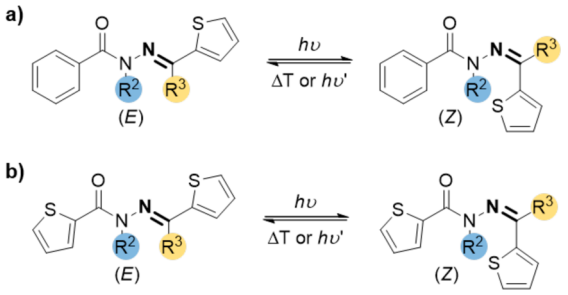

absorbance bands and increases the intensity of the band at lower wavelength ($\lambda_{max} \approx 260$ nm), while the band at higher wavelength ($\lambda_{max} \approx 405$ nm) decreases or disappears, leading to a much lower $\Delta\lambda_{max}$.[17] In addition, the thiophene fingerprint is no longer observed, indicating a loss of rigidity.[21] The thermal half-life on the other hand, increases for R^2 = CH_3, compared to R^2 = H, and even changes T-type (**35** and **36**) photoswitches to P-type (**37** and **38**). We attribute this effect to destabilization of the planar (*E*)-isomer due to increased 1,3-allylic strain resulting in a higher thermal barrier for the less affected nonplanar (*Z*)-isomer. Introducing a Me-group in the R^3-position does not affect the spectral properties significantly when R^2 = H (**35** and **36** compared to **11** and **16**); however, the thermal half-life decreases substantially. Comparing R^3 = H (**33** and **34**) to R^3 = CH_3 (**37** and **38**), while R^2 = CH_3, shows

Table 6. Photochromic Properties of Acylhydrazones Derived from (R^1=) Benzohydrazide (11, 33, 35, and 37) or 2-Thiophenecarboxylic Acid Hydrazide (16, 34, 36, and 38), as a Function of Increasing Steric Bulk in the Hydrazide R^2- and Carbonyl R^3-Positions

compd	R^1	R^2	R^3	λ_{max} [a] [nm]	$\Delta\lambda_{max}$ [b] [nm]	$t_{1/2}$ [c] [min]
11		H	H	319	89	stable
16		H	H	323	90	541
33		CH_3	H	312	55	stable
34		CH_3	H	328	60	stable
35		H	CH_3	312	96	120
36		H	CH_3	322	90	321
37 [d]		CH_3	CH_3	322	0	stable
38 [e]		CH_3	CH_3	334	0	stable

[a]For the (*E*)-isomer. [b]Defined as $\Delta\lambda_{max} = \lambda_{max}(Z) - \lambda_{max}(E)$. [c]At 25 °C; stable photoswitches were defined as those where no thermal *Z*–*E* isomerization was observed for at least 30 min. [d]An increase at λ = 226–287 nm allows for back-isomerization from *Z* to *E* with light (λ_{irr} = 280 nm). [e]The shoulder at λ = 276–304 nm allows for back-isomerization from *Z* to *E* with light (λ_{irr} = 297 nm).

that the long wavelength absorbance band is hypsochromically shifted, leading to lower band separations. All acylhydrazones in Table 6, bearing either one or two Me-moieties in the R^2- and/or R^3-positions, can be reversibly switched between the (*E*)- and (*Z*)-isomers and display clean photoreactions. This proves that while both addressability and thermal stability may be altered by introducing steric bulk or by removing the hydrazone N–H functionality, switching is not inhibited in any case.

CONCLUSIONS

After discussing the correlations of all different substituents and the photochemical properties of this new family of photochromic molecules, and in order to visualize key performance parameters, in particular λ_{max}, $t_{1/2}$, and $\Delta\lambda_{max}$, a graphical, multidimensional representation was chosen to encompass all acylhydrazone photoswitches in the current library (Figure 8). Spheres were colorized with a gradient from red to blue according to their $t_{1/2}$, and the absolute values of λ_{max} (*X*-axis), $t_{1/2}$ (*Y*-axis), and $\Delta\lambda_{max}$ (*Z*-axis) are projected on the respective axes in yellow, orange, and cyan colors. Figure 8 presents a visualization of all acylhydrazones presented in this work and shows that the current collection of acylhydrazone photoswitches covers an extensive range of all parameters, displaying a wide variation in band separation, thermal half-lives, and absorbance maxima, thereby offering a novel, profoundly tunable class of photoswitches.

DOI: 10.1021/jacs.5b09519
J. Am. Chem. Soc. 2015, 137, 14982–14991

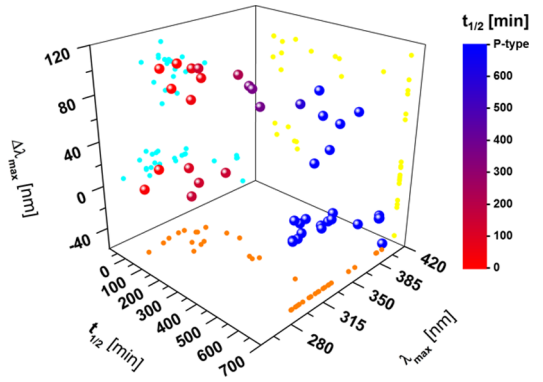

Figure 8. Graphical representation of the acylhydrazone library presented in this work and their position in a 3D-plot with respect to thermal half-life ($t_{1/2}$ on *X*-axis, projection: yellow circles), absorption maximum/excitation wavelength (λ_{max} on *Y*-axis, projection: orange circles), and band separation ($\Delta\lambda_{max}$ on *Z*-axis, projection: teal circles). Spheres are colorized with a gradient according to their $t_{1/2}$ (red to blue).

In summary, a library of over 40 acylhydrazone photoswitches with a broad range of different properties, depending on their substituents, was readily prepared by an easy and modular synthesis and subsequently analyzed. Their addressability by light is highly tunable and excellent band separation of the isomers with large differences of over 100 nm as well as access to both negative and positive photochromic systems was obtained. Both hypsochromic and bathochromic shifts can be induced upon isomerization of the (*E*)- to the (*Z*)-isomer, depending on the particular structure of the photoswitch. Importantly, their thermal stability can be controlled and properties span the entire scale from P-type to T-type chromophores, without the need to specifically stabilize the (*Z*)-isomer, and with tunable half-lives ranging from minutes to several hours for the T-type photoswitches. Moreover, a wide variety of moieties, such as electron-withdrawing and -donating, large aromatic and heteroaromatic groups could be introduced without inhibiting the photochromic function, which opens the door to a myriad of applications for these photoswitches.

Current work in our laboratories is aiming to further bathochromically shift the absorbance maxima and to increase the amount of (*Z*)-isomer in the photostationary state. Importantly, we are actively trying to integrate this new class of photoswitches into our design of remote-controlled catalytic and (supra)molecular systems.

■ ASSOCIATED CONTENT

Supporting Information

The Supporting Information is available free of charge on the ACS Publications website at DOI: 10.1021/jacs.5b09519.

Experimental details, ^{1}H and ^{13}C NMR spectra and UV/vis absorption spectra for all compounds, fatigue resistance, photostationary state and quantum yield determinations (PDF)

■ AUTHOR INFORMATION

Corresponding Author

*sh@chemie.hu-berlin.de

Present Address

‡P.K.: J. Heyrovsky Institute of Physical Chemistry, Academy of Sciences of the Czech republic, Dolejškova 2155/3, 18223 Prague 8, Czech republic.

Author Contributions

†D.J.v.D. and P.K. contributed equally.

Notes

The authors declare no competing financial interest.

■ ACKNOWLEDGMENTS

We thank Dr. A. Goulet-Hanssens, M. Kathan, and S. Fredrich for insightful comments and useful discussions. Generous support by the European Research Council (ERC via ERC-2012-STG_308117 "Light4Function") is gratefully acknowledged. BASF AG, Bayer Industry Services, and Sasol Germany are thanked for generous donations of chemicals.

■ REFERENCES

(1) (a) Beharry, A. A.; Woolley, G. A. *Chem. Soc. Rev.* **2011**, *40*, 4422−4437. (b) Szymański, W.; Beierle, J. M.; Kistemaker, H. A. V.; Velema, W. A.; Feringa, B. L. *Chem. Rev.* **2013**, *113*, 6114−6178. (c) Broichhagen, J.; Trauner, D. *Curr. Opin. Chem. Biol.* **2014**, *21*, 121−127.

(2) For reviews, see: (a) Goulet-Hanssens, A.; Barrett, C. J. *J. Polym. Sci., Part A: Polym. Chem.* **2013**, *51*, 3058−3070. (b) Broichhagen, J.; Frank, J. A.; Trauner, D. *Acc. Chem. Res.* **2015**, *48*, 1947−1960. (c) Velema, W. A.; Szymanski, W.; Feringa, B. L. *J. Am. Chem. Soc.* **2014**, *136*, 2178−2191. Two representative examples include: (d) Schönberger, M.; Althaus, M.; Fronius, M.; Clauss, W.; Trauner, D. *Nat. Chem.* **2014**, *6*, 712−719. (e) Koçer, A.; Walko, M.; Feringa, B. L. *Nat. Protoc.* **2007**, *2*, 1426−1437.

(3) For comprehensive reviews, see: (a) *Molecular Switches*; Feringa, B. L., Browne, W. R., Eds.; John Wiley & Sons: Weinheim, Germany, 2011. (b) Irie, M.; Fukaminato, T.; Matsuda, K.; Kobatake, S. *Chem. Rev.* **2014**, *114*, 12174−12277. (c) Göstl, R.; Senf, A.; Hecht, S. *Chem. Soc. Rev.* **2014**, *43*, 1982−1996. (d) Stoll, R. S.; Hecht, S. *Angew. Chem., Int. Ed.* **2010**, *49*, 5054−5075. Representative examples include: (e) Khan, A.; Kaiser, C.; Hecht, S. *Angew. Chem., Int. Ed.* **2006**, *45*, 1878−1881. (f) Stoll, R. S.; Peters, M. V.; Kuhn, A.; Heiles, S.; Goddard, R.; Bühl, M.; Thiele, C. M.; Hecht, S. *J. Am. Chem. Soc.* **2009**, *131*, 357−367. (g) van Dijken, D. J.; Beierle, J. M.; Stuart, M. C. A.; Szymański, W.; Browne, W. R.; Feringa, B. L. *Angew. Chem., Int. Ed.* **2014**, *53*, 5073−5077. (h) Lohse, M.; Nowosinski, K.; Traulsen, N. L.; Achazi, A. J.; von Krbek, L. K. S.; Paulus, B.; Schalley, C. A.; Hecht, S. *Chem. Commun.* **2015**, *51*, 9777−9780.

(4) (a) Zhang, J.; Zou, Q.; Tian, H. *Adv. Mater.* **2013**, *25*, 378−399. (b) Fihey, A.; Perrier, A.; Browne, W. R.; Jacquemin, D. *Chem. Soc. Rev.* **2015**, *44*, 3719−3759. (c) Abendroth, J. M.; Bushuyev, O. S.; Weiss, P. S.; Barrett, C. J. *ACS Nano* **2015**, *9*, 7746−7768. (d) Russew, M.-M.; Hecht, S. *Adv. Mater.* **2010**, *22*, 3348−3360.

(5) For a concise review, consult: (a) Klajn, R. *Pure Appl. Chem.* **2010**, *82*, 2247−2279. Representative examples include: (b) van der Molen, S. J.; Liljeroth, P. *J. Phys.: Condens. Matter* **2010**, *22*, 133001. (c) Alemani, M.; Peters, M. V.; Hecht, S.; Rieder, K.-H.; Moresco, F.; Grill, L. *J. Am. Chem. Soc.* **2006**, *128*, 14446−14447. (d) Dri, C.; Peters, M. V.; Schwarz, J.; Hecht, S.; Grill, L. *Nat. Nanotechnol.* **2008**, *3*, 649−653. (e) Orgiu, E.; Crivillers, N.; Herder, M.; Grubert, L.; Pätzel, M.; Frisch, J.; Pavlica, E.; Duong, D. T.; Bratina, G.; Salleo, A.; Koch, N.; Hecht, S.; Samorì, P. *Nat. Chem.* **2012**, *4*, 675−679. (f) Gemayel, M. E.; Börjesson, K.; Herder, M.; Duong, D. T.; Hutchison, J. A.; Ruzié, C.; Schweicher, G.; Salleo, A.; Geerts, Y.; Hecht, S.; Orgiu, E.; Samorì, P. *Nat. Commun.* **2015**, *6*, 6330. (g) Bonacchi, S.; El Garah, M.; Ciesielski, A.; Herder, M.; Conti, S.; Cecchini, M.; Hecht, S.; Samorì, P. *Angew. Chem., Int. Ed.* **2015**, *54*, 4865−4869.

(6) (a) Bandara, H. M. D.; Burdette, S. C. *Chem. Soc. Rev.* **2012**, *41*, 1809−1825. (b) Waldeck, D. H. *Chem. Rev.* **1991**, *91*, 415−436.

DOI: 10.1021/jacs.5b09519
J. Am. Chem. Soc. 2015, 137, 14982−14991

(7) (a) Berkovic, G.; Krongauz, V.; Weiss, V. *Chem. Rev.* **2000**, *100*, 1741−1754. (b) Klajn, R. *Chem. Soc. Rev.* **2014**, *43*, 148−184.
(8) (a) Chaur, M. N.; Collado, D.; Lehn, J.-M. *Chem. - Eur. J.* **2011**, *17*, 248−258. (b) Vantomme, G.; Hafezi, N.; Lehn, J.-M. *Chem. Sci.* **2014**, *5*, 1475−1483. (c) Vantomme, G.; Jiang, S.; Lehn, J.-M. *J. Am. Chem. Soc.* **2014**, *136*, 9509−9518. (d) Lehn, J.-M. *Chem. - Eur. J.* **2006**, *12*, 5910−5915. (e) Greb, L.; Lehn, J.-M. *J. Am. Chem. Soc.* **2014**, *136*, 13114−13117.
(9) (a) Ray, D.; Foy, J. T.; Hughes, R. P.; Aprahamian, I. *Nat. Chem.* **2012**, *4*, 757. (b) Su, X.; Lõkov, M.; Kütt, A.; Leito, I.; Aprahamian, I. *Chem. Commun.* **2012**, *48*, 10490−10492. (c) Qian, H.; Aprahamian, I. *Chem. Commun.* **2015**, *51*, 11158−11161.
(10) For comprehensive reviews, see: (a) Rowan, S. J.; Cantrill, S. J.; Cousins, G. R. L.; Sanders, J. K. M.; Stoddart, J. F. *Angew. Chem., Int. Ed.* **2002**, *41*, 898−952. (b) Corbett, P. T.; Leclaire, J.; Vial, L.; West, K. R.; Wietor, J.-L.; Sanders, J. K. M.; Otto, S. *Chem. Rev.* **2006**, *106*, 3652−3711. (c) Belowich, M. E.; Stoddart, J. F. *Chem. Soc. Rev.* **2012**, *41*, 2003−2024. A nice example is given in: (d) Buchs, B.; Fieber, W.; Vigouroux-Elie, F.; Sreenivasachary, N.; Lehn, J.-M.; Herrmann, A. *Org. Biomol. Chem.* **2011**, *9*, 2906−2919.
(11) (a) Su, X.; Aprahamian, I. *Chem. Soc. Rev.* **2014**, *43*, 1963−1981. (b) Tatum, L. A.; Su, X.; Aprahamian, I. *Acc. Chem. Res.* **2014**, *47*, 2141−2149.
(12) Landge, S. M.; Tkatchouk, E.; Benítez, D.; Lanfranchi, D. A.; Elhabiri, M.; Goddard, W. A.; Aprahamian, I. *J. Am. Chem. Soc.* **2011**, *133*, 9812−9823.
(13) Belov, D. G.; Rogachev, B. G.; Tkachenko, L. I.; Smirnov, V. A.; Aldoshin, S. M. *Russ. Chem. Bull.* **2000**, *49*, 666−668.
(14) Ratjen, L.; Lehn, J.-M. *RSC Adv.* **2014**, *4*, 50554−50557.
(15) Asanuma, H.; Liang, X.; Nishioka, H.; Matsunaga, D.; Liu, M.; Komiyama, M. *Nat. Protoc.* **2007**, *2*, 203−212.
(16) Bléger, D.; Hecht, S. *Angew. Chem., Int. Ed.* **2015**, *54*, 11338−11349.
(17) Full characterization and spectroscopic evaluation of all compounds can be found in the Supporting Information.
(18) (a) Matsushima, R.; Nishiyama, M.; Doi, M. *J. Photochem. Photobiol., A* **2001**, *139*, 63−69. (b) Li, X.; Li, J.; Wang, Y.; Matsuura, T.; Meng, J. *J. Photochem. Photobiol., A* **2004**, *161*, 201−213.
(19) (a) Irie, M.; Lifka, T.; Uchida, K.; Kobatake, S.; Shindo, Y. *Chem. Commun.* **1999**, *8*, 747−750. (b) Shoji, H.; Kobatake, S. *Chem. Commun.* **2013**, *49*, 2362−2364. (c) Higashiguchi, K.; Matsuda, K.; Yamada, T.; Kawai, T.; Irie, M. *Chem. Lett.* **2000**, *29*, 1358−1359.
(20) Herder, M.; Schmidt, B. M.; Grubert, L.; Pätzel, M.; Schwarz, J.; Hecht, S. *J. Am. Chem. Soc.* **2015**, *137*, 2738−2747.
(21) Lepeltier, M.; Lukoyanova, O.; Jacobson, A.; Jeeva, S.; Perepichka, D. F. *Chem. Commun.* **2010**, *46*, 7007−7009.
(22) Bouas-Laurent, H.; Dürr, H. *Pure Appl. Chem.* **2001**, *73*, 639−665.
(23) Chandross, E. A.; Ferguson, J.; McRae, E. G. *J. Chem. Phys.* **1966**, *45*, 3546−3553.
(24) (a) Jaunet-Lahary, T.; Chantzis, A.; Chen, K. J.; Laurent, A. D.; Jacquemin, D. *J. Phys. Chem. C* **2014**, *118*, 28831−28841. (b) Knie, C.; Utecht, M.; Zhao, F.; Kulla, H.; Kovalenko, S.; Brouwer, A. M.; Saalfrank, P.; Hecht, S.; Bléger, D. *Chem. - Eur. J.* **2014**, *20*, 16492−16501. (c) Bléger, D.; Schwarz, J.; Brouwer, A. M.; Hecht, S. *J. Am. Chem. Soc.* **2012**, *134*, 20597−20600.
(25) (a) Velema, W. A.; van der Berg, J. P.; Hansen, M. J.; Szymanski, W.; Driessen, A. J. M.; Feringa, B. L. *Nat. Chem.* **2013**, *5*, 924−928. (b) Hansen, M. J.; Velema, W. A.; de Bruin, G.; Overkleeft, H. S.; Szymanski, W.; Feringa, B. L. *ChemBioChem* **2014**, *15*, 2053−2057. (c) Velema, W. A.; van der Toorn, M.; Szymanski, W.; Feringa, B. L. *J. Med. Chem.* **2013**, *56*, 4456−4464. (d) Kienzler, M. A.; Reiner, A.; Trautman, E.; Yoo, S.; Trauner, D.; Isacoff, E. Y. *J. Am. Chem. Soc.* **2013**, *135*, 17683−17686.

DOI: 10.1021/jacs.5b09519
J. Am. Chem. Soc. 2015, 137, 14982−14991